

## Operating principles of Notch–Delta–Jagged module of cell–cell communication

This content has been downloaded from IOPscience. Please scroll down to see the full text.

2015 New J. Phys. 17 055021

(<http://iopscience.iop.org/1367-2630/17/5/055021>)

View [the table of contents for this issue](#), or go to the [journal homepage](#) for more

Download details:

IP Address: 99.72.145.51

This content was downloaded on 13/09/2015 at 05:06

Please note that [terms and conditions apply](#).



## PAPER

## Operating principles of Notch–Delta–Jagged module of cell–cell communication

## OPEN ACCESS

## RECEIVED

14 November 2014

## REVISED

21 March 2015

## ACCEPTED FOR PUBLICATION

15 April 2015

## PUBLISHED

20 May 2015

Content from this work  
may be used under the  
terms of the [Creative  
Commons Attribution 3.0  
licence](#).

Any further distribution of  
this work must maintain  
attribution to the  
author(s) and the title of  
the work, journal citation  
and DOI.



Mohit Kumar Jolly<sup>1,2,8</sup>, Marcelo Boareto<sup>1,7,8</sup>, Mingyang Lu<sup>1</sup>, Jose' N Onuchic<sup>1,3,4,5</sup>, Cecilia Clementi<sup>1,3</sup> and Eshel Ben-Jacob<sup>1,5,6</sup>

<sup>1</sup> Center for Theoretical Biological Physics, Rice University, Houston, TX 77005-1827, USA

<sup>2</sup> Department of Bioengineering, Rice University, Houston, TX 77005-1827, USA

<sup>3</sup> Department of Chemistry, Rice University, Houston, TX 77005-1827, USA

<sup>4</sup> Department of Physics and Astronomy, Rice University, Houston, TX 77005-1827, USA

<sup>5</sup> Department of Biosciences, Rice University, Houston, TX 77005-1827, USA

<sup>6</sup> School of Physics and Astronomy and The Sagol School of Neuroscience, Tel-Aviv University, Tel-Aviv 69978, Israel

<sup>7</sup> Institute of Physics, University of Sao Paulo, Sao Paulo 05508, Brazil

<sup>8</sup> These authors made equal contribution.

E-mail: [jonuchic@rice.edu](mailto:jonuchic@rice.edu), [cecilia@rice.edu](mailto:cecilia@rice.edu) and [eshelbj@gmail.com](mailto:eshelbj@gmail.com)

**Keywords:** notch signaling, multistability, jagged, sender/receiver, cell–cell communication, pattern formation

Supplementary material for this article is available [online](#)

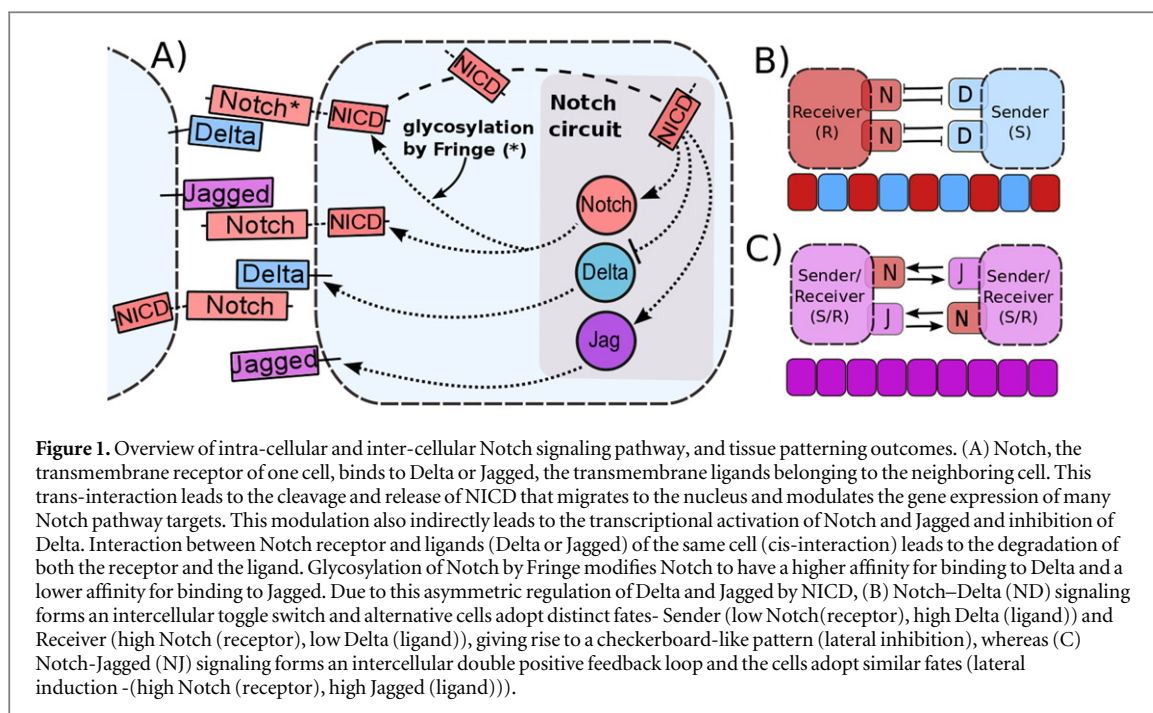
## Abstract

Notch pathway is an evolutionarily conserved cell–cell communication mechanism governing cell-fate during development and tumor progression. It is activated when Notch receptor of one cell binds to either of its ligand—Delta or Jagged—of another cell. Notch–Delta (ND) signaling forms a two-way switch, and two cells interacting via ND signaling adopt different fates—Sender (high ligand, low receptor) and Receiver (low ligand, high receptor). Notch–Delta–Jagged signaling (NDJ) behaves as a three-way switch and enables an additional fate—hybrid Sender/Receiver (S/R) (medium ligand, medium receptor). Here, by extending our framework of NDJ signaling for a two-cell system, we show that higher production rate of Jagged, but not that of Delta, expands the range of parameters for which both cells attain the hybrid S/R state. Conversely, glycosyltransferase Fringe and *cis*-inhibition reduces this range of conditions, and reduces the relative stability of the hybrid S/R state, thereby promoting cell-fate divergence and consequently lateral inhibition-based patterns. Lastly, soluble Jagged drives the cells to attain the hybrid S/R state, and soluble Delta drives them to be Receivers. We also discuss the critical role of hybrid S/R state in promoting cancer metastasis by enabling collective cell migration and expanding cancer stem cell (CSC) population.

## Introduction

Biological systems comprise of many interconnected networks operating at different scales—from genetic and sub-cellular level to inter-cellular communication at tissue level to interactions among organ systems. At sub-cellular level, gene regulatory networks (GRNs) govern the cell-fate decisions and coordinate them via cell–cell communication, thereby giving rise to different patterns at a tissue level; whereas at organ level, dynamic physiological networks underlie the emergent behavior of the system [1–3].

Elucidating the ‘operating principles’ or the relationship between the topology and function of these networks is instrumental in addressing a key challenge in modern developmental and cancer biology—understanding cell-fate decisions during embryonic development and tumor initiation and progression. Recently, rapid progress has been witnessed in mapping the GRNs associated with such decisions in multiple contexts [4]. Cellular decision making in these examples involve changes in the expression of various transcription factors (TFs), microRNAs (miRNAs) and GTPases that regulate cascades of regulatory networks, ultimately giving rise to global gene expression patterns and protein levels that correspond to a specific cell lineage (fate) [5].



Cell–cell communication, a crucial component of decision making, allows coordinating the fate decisions of a population of cells, such as the decision to sporulate or not in bacteria [6]. A key evolutionarily conserved cell–cell communication pathway that coordinates cell-fate decision both during embryonic development and tumor progression is the Notch signaling pathway. This pathway consists of the transmembrane receptor Notch and the transmembrane ligands Delta and Jagged. In mammals, there are four Notch receptors (Notch1–4) and five ligands (Jag1, Jag2, Delta-like 1 (Dll1), Dll3 and Dll4). When Notch (any of the four members) of one cell interacts with Delta or Jagged (any of the five members) of the same cell, it leads to degradation of both of them; this mechanism is known as *cis*-inhibition. Conversely, when Notch of one cell interacts with Delta or Jagged of the neighboring cell, this interaction cleaves Notch and leads to the release of notch intracellular domain (NICD) into the cytoplasm that later enters the nucleus and activates many downstream target genes. This mechanism, referred to as *trans*-activation, activates the Notch pathway (see [7] for a recent review).

Although Delta and Jagged generate the same signal NICD, the dynamics of Notch–Delta (ND) and Notch–Jagged (NJ) signaling are quite different, because NICD regulates the production of the two ligands asymmetrically—it inhibits Delta but activates Jagged (figure 1(A)). Therefore, Notch and Delta form an intercellular double negative feedback loop, but Notch and Jagged form an intercellular double positive feedback loop. Consequently, the two cells interacting via ND adopt different fates—one cell behaves as a Sender (S) with (high Delta (ligand), low Notch (receptor)) on its surface; and the other behaves as a Receiver (R) with (low Delta (ligand), high Notch (receptor)) on its surface. This cell-fate diversification mechanism is known as lateral inhibition and can lead to checkerboard-like or ‘salt-and-pepper’ patterns (figure 1(B)) as observed during bristle patterning in flies, inner ear patterning in vertebrates, and neurogenesis in both flies and vertebrates (see [8] for a recent review). On the other hand, two cells interacting via NJ can act as both Sender and Receiver as they have (high Jagged (ligand), high Notch (receptor)) on their surface. This cell-fate convergence mechanism is known as lateral induction (figure 1(C)) and is crucial during cardiac development, inner ear development, and the formation of a smooth muscle wall around a nascent artery [9–12].

Another level of asymmetry that modulates the dynamics of Notch signaling via Delta versus Jagged is the effect of a downstream target of NICD—the glycosyltransferase Fringe [13] that can increase the binding affinity of Notch for Delta, but decrease that for Jagged, both for *cis*- and *trans*-interactions [14–17]. These two levels of asymmetry in ND versus NJ signaling call for elucidating their different operating principles.

It may be noted that unlike Jagged1, Jagged2 behaves similar to Delta [18] and is not activated by NICD. Therefore NJ1, but not necessarily NJ2, forms a double positive feedback loop. Results presented here, hence, are likely to be more consistent with the experimental results for Jagged1.

Most experimental and theoretical efforts have focused on understanding ND signaling [8]. NJ signaling has not received enough attention, despite its crucial role during embryonic development, and promoting tumor progression in multiple ways. Jagged1 can initiate metastasis by inducing cancer cells to undergo epithelial to mesenchymal transition (EMT)—a dormant embryonic program that allows them to migrate and invade. It also

facilitates the colonization of the circulating tumor cells (CTCs) by enabling cell–cell communication between CTCs and the cells of the organ where they settle down and develop metastases [19, 20] that causes more than 90% of cancer-related deaths [21]. Furthermore, NJ signaling can also maintain and/or expand the population of cancer stem cells (CSCs)—highly plastic cancer cells that can initiate a new tumor [22–24], thereby promoting tumor relapse. Not surprisingly, poor survival and cancer recurrence is associated with high levels of Jagged1 in patients [19]. Hence, understanding NJ, and more specifically NJ1, signaling is essential to control tumor spread.

Previously, we developed a theoretical framework that incorporates the effect of both ligands—Delta and Jagged—on Notch signaling [25]. We evaluated the dynamics of Notch, Delta, Jagged and NICD of a single cell by varying a fixed external input to the cell—the amount of Notch, Delta and Jagged of the neighboring cells, i.e. no feedback from adjacent cells was considered. We found that Notch–Delta–Jagged (NDJ) signaling circuit can behave as a three-way switch, giving rise to an additional hybrid Sender/Receiver (S/R)—(medium ligand, medium receptor) through which cells can both send and receive signals, and can adopt similar fates [25]. However, as opposed to the results largely pertaining to a single-cell system, here, we have extended that framework by focusing on a two-cell system (two identical cells interacting via NDJ system) to elucidate the effect of *cis*-inhibition, Fringe, production rates of Delta and Jagged, and soluble ligands in cell fate decisions mediated by the Notch signaling pathway, and cell-fate patterns observed at a tissue level. We show that higher innate production rate of Jagged, but not that of Delta, expands the range of parameters or physiological conditions under which both these cells attain the hybrid S/R state. Conversely, Fringe reduces this range of conditions that enables both cells to adopt similar fate. Both Fringe and *cis*-inhibition reduce the relative stability of the hybrid S/R state and increase that of S and R states, thereby promoting cell-fate divergence and consequently lateral inhibition-based patterns. Further, to elucidate the effect of soluble ligands in cell-fate decision, we found that soluble Jagged drives the cells to attain the hybrid S/R state, and soluble Delta drives them to be Receivers. Lastly, we discuss the critical role that the hybrid S/R state plays in tumor progression—by enabling collective cell migration during cancer metastasis, as well as by expanding the pool of tumor-initiating cells or CSCs that mediate the formation of secondary tumors, as well as tumor relapse.

### Theoretical framework

Our framework has been introduced in [25], that extends previous work [26] by incorporating Jagged in addition to Delta and the asymmetric regulation of the proteins by the signal NICD that activates Notch and Jagged but represses Delta. *Trans*-activation (interaction between receptor of one cell and ligand of the neighboring cell) activates the Notch signaling pathway by releasing the signal (NICD), but *cis*-inhibition (interaction between the receptor and ligand belonging to the same cell) leads to the degradation of both proteins. We initially assume no effect of the glycosyltransferase Fringe, i.e., the affinity of Notch to Delta or Jagged is the same. In this case, the equations for the Notch receptor ( $N$ ), the ligands Delta ( $D$ ) and Jagged ( $J$ ), and the signal NICD ( $I$ ), are given by:

$$\frac{dN}{dt} = N_0 H^{S^+}(I, \lambda_{I,N}) - k_C N [D + J] - k_T N [D_{\text{ext}} + J_{\text{ext}}] - \gamma N, \quad (1)$$

$$\frac{dD}{dt} = D_0 H^{S^-}(I, \lambda_{I,D}) - k_C D N - k_T D N_{\text{ext}} - \gamma D, \quad (2)$$

$$\frac{dJ}{dt} = J_0 H^{S^+}(I, \lambda_{I,J}) - k_C J N - k_T J N_{\text{ext}} - \gamma J, \quad (3)$$

$$\frac{dI}{dt} = k_T N [D_{\text{ext}} + J_{\text{ext}}] - \gamma_I I, \quad (4)$$

where  $N_0$ ,  $D_0$ , and  $J_0$  represent innate production rates of Notch, Delta and Jagged respectively. Their degradation rates have been considered to be the same, represented by  $\gamma$ .  $N_{\text{ext}}$ ,  $D_{\text{ext}}$  and  $J_{\text{ext}}$  are the amounts of receptor Notch, and ligands Delta and Jagged available from neighboring cells.  $k_C$  and  $k_T$  represent the *cis*-inhibition rates and *trans*-activation rates of Notch with its ligands.  $\gamma_I$  denotes the degradation rate of NICD.  $H^{S^+}(I, \lambda_{I,N})$  and  $H^{S^+}(I, \lambda_{I,J})$  represent the transcriptional activation of Notch ( $N$ ) and Jagged ( $J$ ) by the signal NICD ( $I$ ), and  $H^{S^-}(I, \lambda_{I,D})$  denotes the repression of Delta ( $D$ ) by  $I$ .  $H^{S^+}(I, \lambda_{I,N})$ ,  $H^{S^+}(I, \lambda_{I,J})$  and  $H^{S^-}(I, \lambda_{I,D})$  are shifted Hill functions defined as  $H^-(X) + \lambda_{X,Y} H^+(X)$  where  $H^-(X)$  is inhibitory Hill function, and  $H^+(X)$  is excitatory Hill function, and  $\lambda_{X,Y}$  denotes the fold-change in production of  $Y$  due to  $X$ . For activation, shifted Hill functions are depicted by  $H^{S^+}$  and  $\lambda_{X,Y} > 1$ ; for inhibition, they are depicted by  $H^{S^-}$  and  $\lambda_{X,Y} < 1$ .  $\lambda_{X,Y} = 1$  denotes no effect in production rate [27].

NICD (Notch signal) degrades rapidly as compared to  $N$ ,  $D$  and  $J$  [28]. Therefore, we can assume a quasi-steady approximation for it. In this case, equations (1)–(4) can be reduced to two equations by defining  $L = D + J$  and  $L_{\text{ext}} = D_{\text{ext}} + J_{\text{ext}}$ , where  $L$  represents the total amount of both ligands in the cell, and  $L_{\text{ext}}$  denotes the total

amount of external ligands available to bind. Then, the reduced system is:

$$\frac{dN}{dt} = N_0 H^{S+}(I, \lambda_{I,N}) - k_C N L - k_T N L_{\text{ext}} - \gamma N, \quad (5)$$

$$\frac{dL}{dt} = D_0 H^{S-}(I, \lambda_{I,D}) + J_0 H^{S+}(I, \lambda_{I,J}) - k_C L N - k_T L N_{\text{ext}} - \gamma L, \quad (6)$$

where, by quasi steady-state approximation,  $I = k_T N L_{\text{ext}} / \gamma I$ .

Until now, we considered equal *cis*-inhibition rates ( $k_C$ ) as well as equal *trans*-activation rates ( $k_T$ ) for both ligands. However, when we include the effect of Fringe, a downstream target of Notch signaling [13], we consider two populations of Notch—one that is modified (glycosylated) by Fringe and the other that is not (see derivation in SI section S2). The modified Notch has a higher binding affinity for Delta but lower for Jagged as compared to the unmodified one, both in *cis* and in *trans* [14–17]. Now, *cis*-inhibition rates  $k_{C_D}$  and  $k_{C_J}$  and *trans*-activation rates  $k_{T_D}$  and  $k_{T_J}$  depend on the levels of NICD ( $I$ ) that activates Fringe. Thus, when Fringe's effect is incorporated,  $k_{C_D} = k_C H^{S+}(I, \lambda_{F,D})$  and  $k_{T_D} = k_T H^{S+}(I, \lambda_{F,D})$  where  $\lambda_{F,D} > 1$  (Fringe increases the binding of  $N$  to  $D$  and  $D_{\text{ext}}$ ). Similarly, since Fringe decreases the binding of  $N$  to  $J$  and  $J_{\text{ext}}$ ,  $\lambda_{F,J} < 1$  in  $k_{C_J} = k_C H^{S-}(I, \lambda_{F,J})$  and  $k_{T_J} = k_T H^{S-}(I, \lambda_{F,J})$ , and the dynamics of  $N$ ,  $D$ ,  $J$  and  $I$  are given by:

$$\frac{dN}{dt} = N_0 H^{S+}(I, \lambda_{I,N}) - N [k_{C_D} D + k_{C_J} J] - N [k_{T_D} D_{\text{ext}} + k_{T_J} J_{\text{ext}}] - \gamma N, \quad (7)$$

$$\frac{dD}{dt} = D_0 H^{S-}(I, \lambda_{I,D}) - k_{C_D} D N - k_{T_D} D N_{\text{ext}} - \gamma D, \quad (8)$$

$$\frac{dJ}{dt} = J_0 H^{S+}(I, \lambda_{I,J}) - k_{C_J} J N - k_{T_J} J N_{\text{ext}} - \gamma J, \quad (9)$$

$$\frac{dI}{dt} = N [k_{T_D} D_{\text{ext}} + k_{T_J} J_{\text{ext}}] - \gamma I. \quad (10)$$

The effect of Fringe here is given by two independent parameters— $\lambda_{F,D}$  and  $\lambda_{F,J}$ . Later, to elucidate the net effect, we collapse these two parameters into a single parameter ( $f$ ) that represents the Fringe effect such that  $f = \lambda_{F,D} = 1/\lambda_{F,J}$ ,  $f = 1$  represents no effect of Fringe and the higher the value of  $f$ , the stronger is this effect.

Recent studies show that some cells can release soluble form of the ligands Delta and Jagged that activate Notch signaling in the neighbors in a paracrine manner [23, 29]. However, soluble ligands do not have enough mechanical pulling force to cleave Notch and generate NICD [30] and they require alternative mechanisms such as ligand multi-merization to generate sufficient mechanical force [31]. For this reason, soluble ligands are expected to have lower *trans*-activation rates than those of membrane-bound ligands [32]. Therefore, a model that considers both soluble and the membrane-bound ligands should have two terms in equation (7) (Notch equation) for interaction with both forms of these ligands, and equations (7)–(10) would be given by equations (11)–(14), where  $D_{\text{ext}}^s$  and  $J_{\text{ext}}^s$  represent soluble forms of ligands Delta and Jagged respectively, and  $k_{T_D}^s$  and  $k_{T_J}^s$  denote the *trans*-activation rates of Notch signaling for soluble ligands Delta and Jagged, respectively, such that  $k_{T_D}^s = k_T^s H^{S+}(I, \lambda_{F,D})$  and  $k_{T_J}^s = k_T^s H^{S-}(I, \lambda_{F,J})$ .

$$\begin{aligned} \frac{dN}{dt} = & N_0 H^{S+}(I, \lambda_{I,N}) - N [k_{C_D} D + k_{C_J} J] - N [k_{T_D} D_{\text{ext}} + k_{T_J} J_{\text{ext}}] \\ & - N [k_{T_D}^s D_{\text{ext}}^s + k_{T_J}^s J_{\text{ext}}^s] - \gamma N, \end{aligned} \quad (11)$$

$$\frac{dD}{dt} = D_0 H^{S-}(I, \lambda_{I,D}) - k_{C_D} D N - k_{T_D} D N_{\text{ext}} - \gamma D, \quad (12)$$

$$\frac{dJ}{dt} = J_0 H^{S+}(I, \lambda_{I,J}) - k_{C_J} J N - k_{T_J} J N_{\text{ext}} - \gamma J, \quad (13)$$

$$\frac{dI}{dt} = N [k_{T_D} D_{\text{ext}} + k_{T_J} J_{\text{ext}}] + k_{T_D}^s N [D_{\text{ext}}^s + J_{\text{ext}}^s] - \gamma I. \quad (14)$$

For the case of two-cell system interacting solely with each other via NDJ signaling (i.e. the two cells do not respond to any external signal apart from the ligands of the neighboring cell),  $N_{\text{ext}}$ ,  $D_{\text{ext}}$ ,  $J_{\text{ext}}$  represent the Notch, Delta and Jagged respectively of the neighboring cell. The dynamics of cell #1 interacting with cell #2 can be described by equations (15)–(18) (similar equations represent the dynamics of cell #2 interacting with cell #1):

$$\begin{aligned} \frac{dN_1}{dt} = & N_0 H^{S+}(I_1, \lambda_{I,N_1}) - N_1 [(k_C D_1 + k_T D_2) H^{S+}(I_1, \lambda_{F,D}) \\ & + (k_C J_1 + k_T J_2) H^{S-}(I_1, \lambda_{F,J})] - \gamma N_1, \end{aligned} \quad (15)$$

$$\frac{dD_1}{dt} = D_0 H^{S-}(I_1, \lambda_{I,D_1}) - k_C H^{S+}(I_1, \lambda_{F,D}) D_1 N_1 - k_T H^{S+}(I_2, \lambda_{F,D}) N_2 D_1 - \gamma D_1, \quad (16)$$

$$\frac{dJ_1}{dt} = J_0 H^{S+}(I_1, \lambda_{I,J}) - k_C H^{S-}(I_1, \lambda_{F,J}) J_1 N_1 - k_T H^{S-}(I_2, \lambda_{F,J}) N_2 J_1 - \gamma J_1, \quad (17)$$

$$\frac{dI_1}{dt} = k_T N_1 \left[ J_2 H^{S-}(I_1, \lambda_{F,J}) + D_2 H^{S+}(I_1, \lambda_{F,D}) \right] - \gamma I_1, \quad (18)$$

where  $N_1, D_1, J_1$  and  $I_1$  represent the Notch receptor, Delta, Jagged and NICD respectively for cell #1, and similarly  $N_2, D_2, J_2$  and  $I_2$  represent the Notch receptor, Delta, Jagged and NICD respectively for cell #2.

Similarly, the system can be extended to the case where each cell has  $n$ -neighbors, and the generalized equations are given by equations (19)–(22) given as:

$$\frac{dN}{dt} = N_0 H^{S+}(I, \lambda_{I,N}) - N \left[ \left( k_C D + k_T \sum_{i=1}^n D_i \right) H^{S+}(I, \lambda_{F,D}) + \left( k_C J + k_T \sum_{i=1}^n J_i \right) H^{S-}(I, \lambda_{F,J}) \right] - \gamma N, \quad (19)$$

$$\frac{dD}{dt} = D_0 H^{S-}(I, \lambda_{I,D}) - k_C H^{S+}(I, \lambda_{F,D}) D N - k_T D \sum_{i=1}^n N_i H^{S+}(I_i, \lambda_{F,D}) - \gamma D, \quad (20)$$

$$\frac{dJ}{dt} = J_0 H^{S+}(I, \lambda_{I,J}) - k_C H^{S-}(I, \lambda_{F,J}) J N - k_T J \sum_{i=1}^n N_i H^{S-}(I_i, \lambda_{F,J}) - \gamma J, \quad (21)$$

$$\frac{dI}{dt} = k_T N \sum_{i=1}^n \left[ J_i H^{S-}(I, \lambda_{F,J}) + D_i H^{S+}(I, \lambda_{F,D}) \right] - \gamma I. \quad (22)$$

A detailed discussion of the values of the parameters used is presented in the SI section S1 (available at [stacks.iop.org/NJP/17/055021/mmedia](http://stacks.iop.org/NJP/17/055021/mmedia)). The model is robust with respect to changes in the values of the most parameters as discussed in the section S3 in the SI, and is most sensitive to the production and degradation rates of Notch ( $N_0$  and  $\gamma$  respectively), production rate of Delta  $D_0$ , and the trans-activation rate  $k_T$ . The codes were implemented in python using the PyDSTool [33].

## Cell fate decisions in ND, NJ and NDJ signaling circuits

### ND signaling circuit

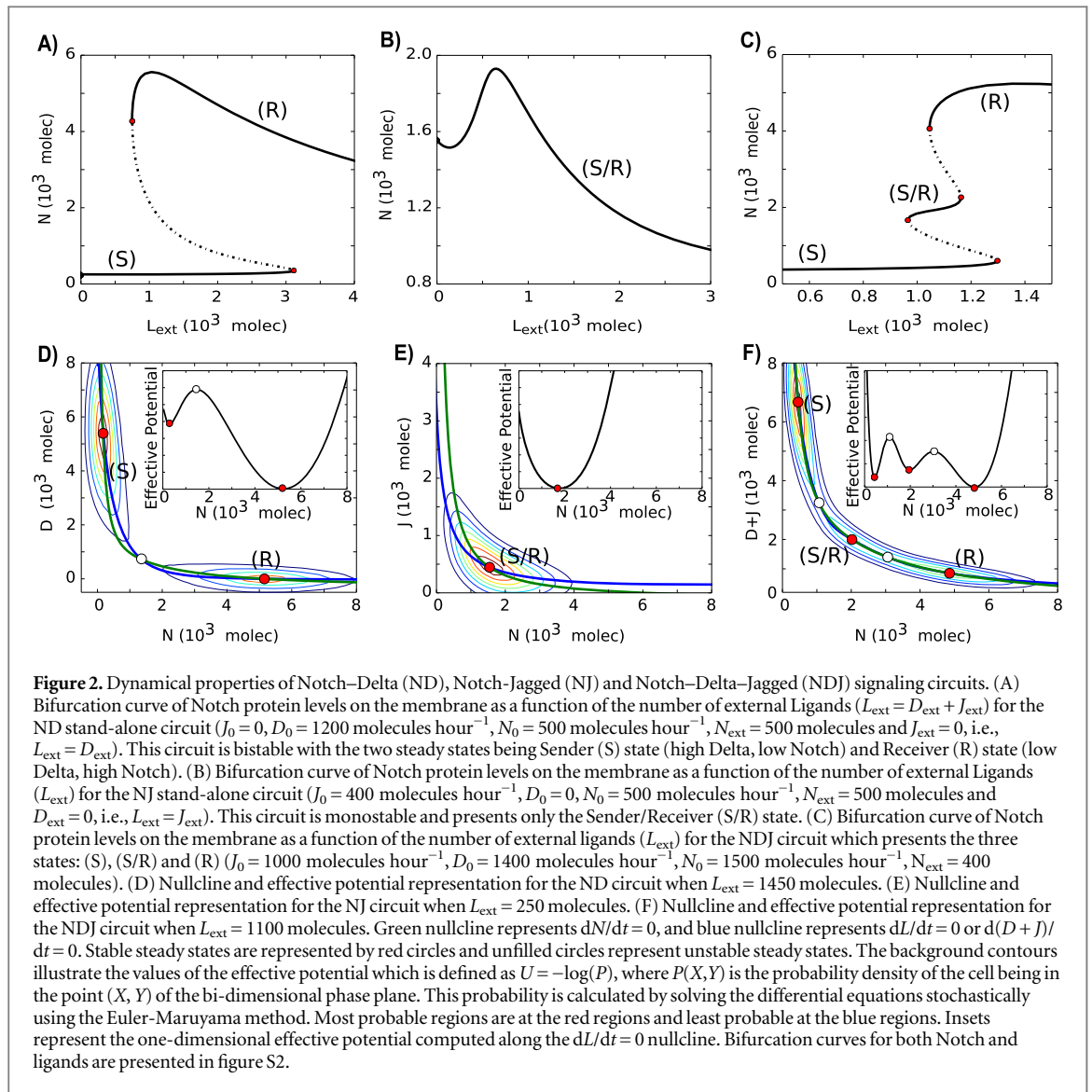
We first evaluate the dynamics of ND signaling for one-cell system by analyzing the reduced model given by equations (5)–(6) when  $J_0 = 0$ , i.e., no Jagged is produced. In this case, ND circuit is bistable, and the two stable steady states are:—(i) Sender (S)—in which the cell has (high Delta (ligand), low Notch (receptor)), and (ii) Receiver (R)—in which the cell has (low Delta (ligand), high Notch (receptor)) (figures 2(A) and (D)). Low levels of Delta in the neighboring cell ( $D_{\text{ext}}$ ) cause the cell to behave as a Receiver (low Delta, high Notch), while high levels of  $D_{\text{ext}}$  cause it to behave as a Sender (high Delta, low Notch), i.e. the two adjacent cells adopt alternate fates (figure 2(A)). However, at intermediate levels of  $D_{\text{ext}}$ , we see a coexistence of the Sender and Receiver states, such that random fluctuations in the cell can lead to a transition between the states or a switching of the cell-fate (figure 2(D)).

This switch-like behavior of ND signaling has been noted in previous studies as well [26, 34, 35]. A canonical example of this phenomenon, also known as lateral inhibition, is the AC/VU differentiation in *C. elegans*, where initially the two cells are identical (i.e. both neighbors have the same levels of ligand and receptor), but due to a random fluctuation, one cell has increased levels of ligand and/or the other has increased levels of receptor; and this stochastic difference is amplified by the mutually inhibitory feedback loop—thereby driving the cell fate diversification [34]. However, lateral inhibition need not be static, it can be dynamic too—i.e. cells can compete against their neighbors continuously, as seen during sprouting angiogenesis, where the migrating ‘stalk’ cells are continuously competing to become ‘tip’ cells [36]. Also, during neural development, lateral inhibition occurs between the dynamic clusters of neuronal precursors, in order to strike a balance between the number of cells differentiating to become neurons, and those staying as precursors for further rounds of neurogenesis [37].

In addition to alternate fate or checkerboard-like patterns, lateral inhibition can also give rise to sparse or non-checkerboard patterns, i.e. patterns with a spacing of more than one cell, when the cooperativity (Hill function coefficient) in interaction between Notch and Delta of adjacent cells is weak, or when the ND system is expanded to consider other molecules such as miR-124 [35, 38].

### NJ signaling circuit

We next consider the dynamics of NJ signaling for one-cell system by analyzing the reduced model given by equations (5)–(6) when  $D_0 = 0$ , i.e., no Delta is produced. NJ circuit is monostable with the only steady state being when cells have (medium Jagged (ligand), medium Notch (receptor)) (figures 2(B) and (E)), thus cells can

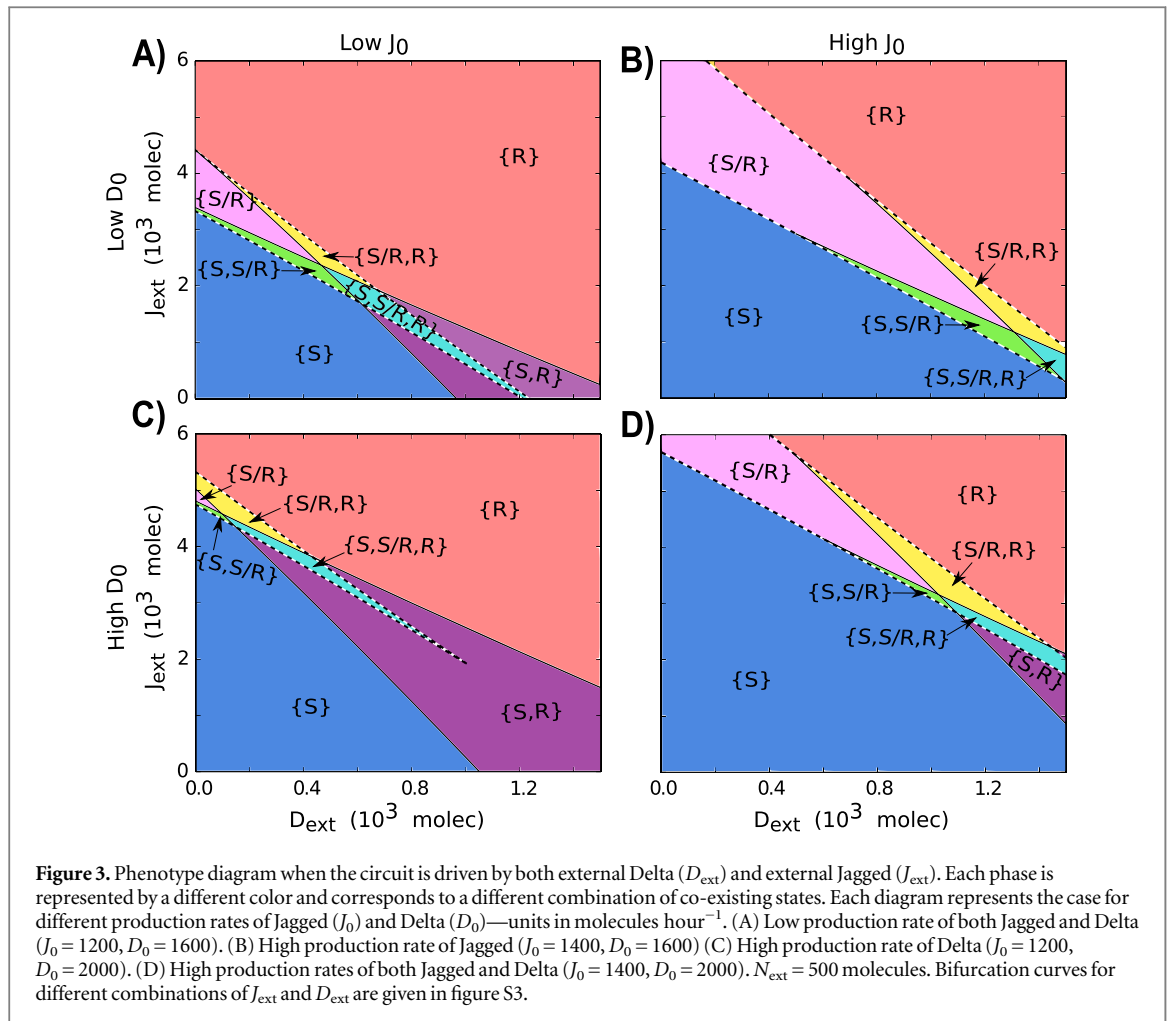


both send and receive signals, thereby leading to cell fate convergence. This phenomenon, also known as lateral induction, can also play a crucial role in generating spatial patterns with wavelength of a dozen of cells [39], and can thereby facilitate the spatial patterning of different cell types required during pancreatic development [40]. Since previous computational models for lateral induction [39, 40] do not specifically consider Jagged, they can offer limited insights into cases where Jagged plays a key role, such as in tumor–stroma crosstalk [22, 23]. A recent model of Notch signaling in inner ear development explores the effect of both Delta and Jagged in Notch signaling [10], however, *cis*-inhibition between Notch and its ligands was not included in the model, because it does not occur in this biological context. Nonetheless, it (*cis*-inhibition) can indeed be crucial in Notch signaling functioning in other biological contexts, and can affect cell–fate decisions and patterning [14, 41, 42].

#### NDJ signaling circuit

We next study the dynamics of the combined NDJ signaling, i.e., Notch signaling when driven by both its ligands—Delta and Jagged. This system can behave as a three-way switch, allowing for three states:—(i) Sender (S—high ligand, low receptor), (ii) Receiver (R—low ligand, high receptor) and (iii) hybrid Sender/Receiver (S/R—medium ligand, medium receptor). In this case, for a small range of  $L_{\text{ext}}$ , the three steady states coexist and random fluctuations can lead to a transition between the states (figure 2(C) and (F)). Such multistability has also been observed in many other contexts related to cell–fate decisions at a sub-cellular level [27, 43–47].

A computational model that includes both ligands Delta and Jagged, and also their *cis*-interactions with Notch can be crucial to understand the developmental systems where both lateral inhibition and lateral induction are acting simultaneously, such as during angiogenesis and pancreatic cell differentiation. During angiogenesis, Jagged mediates the number of ‘stalk’ cells that may separate two ‘tip’ cells [48], and the three fates that can be obtained in the context of NDJ signaling may underlie the highly dynamic phenotypes that

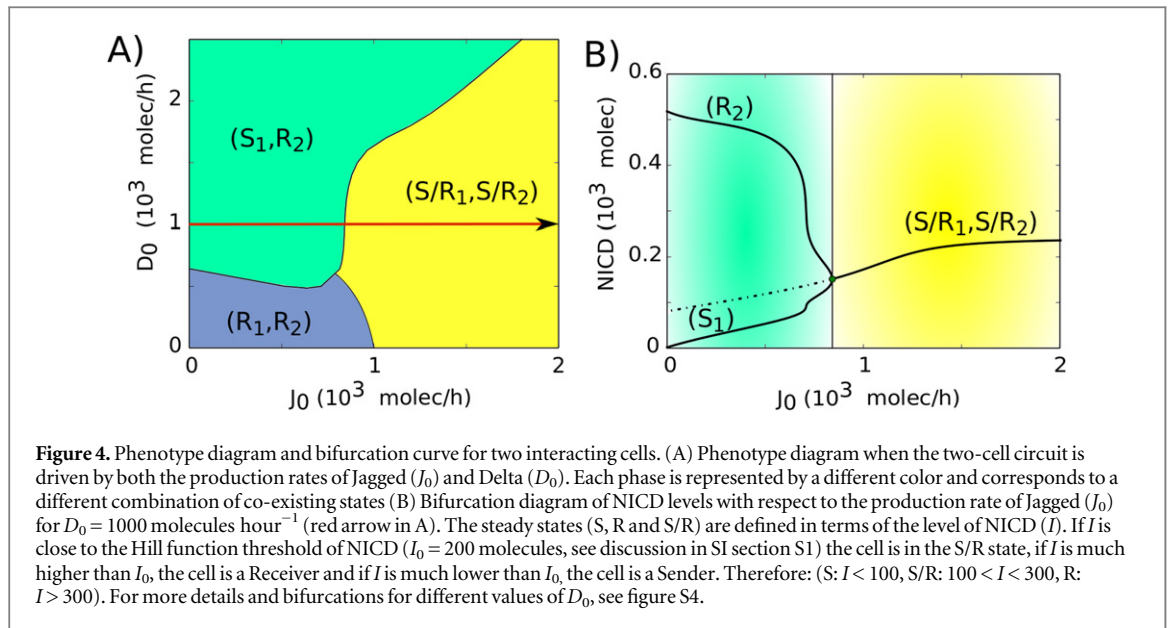


endothelial cells can attain that are neither entirely either tip nor stalk [49]. Both lateral inhibition and lateral induction are also critical for multistability of the pancreatic system, wherein the loss of either of them can lead to lineage switching between various cell types [50].

### Production rates of the two ligands affect cell-fate decision antagonistically

The two ligands—Delta and Jagged—can be produced at different rates in the same cell due to stochastic events and/or the influence of external factors such as the inflammatory cytokine TNF- $\alpha$  that can promote the production of Jagged and inhibit that of Delta [48]. Therefore, we next explore the effect of varying the production rates of the ligands on cell-fate decisions mediated by NDJ signaling, for both a one-cell and a two-cell system. For the one-cell system, our results are represented as phenotype diagrams when the circuit is driven by two control parameters—external Delta ( $D_{\text{ext}}$ ) and external Jagged ( $J_{\text{ext}}$ ) (figure 3). Until now, we have considered the total amount of external ligands ( $L_{\text{ext}} = D_{\text{ext}} + J_{\text{ext}}$ ) driving the circuit, but now we consider the two ligands  $D_{\text{ext}}$  and  $J_{\text{ext}}$  separately so as to incorporate the effect of Fringe that creates an asymmetry between the likelihood of Notch to interact with these two ligands. The circuit now is represented by equations (7)–(10). These diagrams consist of multiple phases (sets of co-existing phenotypes for the same parameter set): three monostable phases—{S}, {S/R} and {R}, three bistable phases—{S, R}, {S, S/R} and {S/R, R}, and a tristable phase—{S, S/R, R}.

Different phenotype diagrams denote different combinations of the production rates of Jagged and Delta. At low production rates of Jagged ( $J_0$ ), the increase in production rate of Delta ( $D_0$ ) decreases the parameter range for the existence of phases containing the hybrid S/R phenotype (compare the area bounded by dashed lines in figure 3(C) versus that in figure 3(A)). Similar effects of high production rates of Delta ( $D_0$ ) are observed at high production rates of Jagged ( $J_0$ ) (compare the area bounded by dashed lines in figure 3(D) versus that in figure 3(B)). Therefore, high levels of Delta inhibit NJ signaling and promote lateral inhibition or cell fate diversification. Conversely, high production rates of Jagged can significantly increase the parameter range for the existence of phases containing the hybrid S/R phenotype, and this effect is more pronounced at low production



rates of Delta (compare the area bounded by dashed lines in figure 3(B) vs. that in figure 3(A). Hence, the two ligands act antagonistically with respect to their effect on cell-fate decisions in a cell population.

Next, we investigate the effect of different production rates of Delta ( $D_0$ ) and Jagged ( $J_0$ ) in a two-cell system. Both these cells are identical and communicate with each other via the NDJ system. At low production rates of both ligands (Jagged and Delta) in both cells, they act as Receiver ( $R_1, R_2$ )—low ligand, high receptor) because Notch (receptor) is still being produced at a fixed rate. However, when the production rate of Delta is higher than that of Jagged, one cell becomes the Sender (S) and the other the Receiver (R)—( $S_1, R_2$ ) or ( $R_1, S_2$ ). Conversely, when the production rate of Jagged is higher than that of Delta, both cells attain the hybrid S/R state that enables them to communicate in a bidirectional manner via the NDJ system ( $S/R_1, S/R_2$ ) (figures 4 and S4). Consistent with these results for a two-cell system, the different production rates of these ligands can also have opposite effects on the emergent tissue-level patterning. High production rates of Delta, but not that of Jagged, can facilitate checkerboard-like ‘salt-and-pepper’ pattern [25].

### Effect of Fringe on cell-fate dynamics

In *Drosophila* as well as mammals, Fringe can promote ND signaling by increasing the binding affinity of Notch for Delta and decreasing that for Jagged, both for *cis*-inhibition and *trans*-activation interactions [14, 15]. Here, for both one-cell and two-cell systems, we explore how Fringe levels affect the parameter range for attaining the different steady states in NDJ circuit and their relative stability. We consider the effect of Fringe on NDJ signaling by a single variable  $f$ , such that  $f = \lambda_{F,D} = 1/\lambda_{F,J}$ , where  $\lambda_{F,D}$  and  $\lambda_{F,J}$  denote the fold-change in binding affinity (or equivalently the *cis*-inhibition and *trans*-activation rates) between (Notch and Delta) and (Notch and Jagged) respectively.

#### Fringe promotes lateral inhibition patterning

For one-cell system, we investigate the effect of Fringe when it is driven exclusively by different levels of  $D_{\text{ext}}$  and  $J_{\text{ext}}$ . We plot a bifurcation diagram for the Fringe effect and the external ligand driving the cell, and find that an increase in Fringe effect decreases the range of existence of the phases that contain the hybrid S/R state—{S/R}, {S, S/R}, {S/R, R} and {S, S/R, R} (figure S5), thereby being consistent with the NJ signaling attenuating role of Fringe. We next address the effect of Fringe on tissue patterning by simulating a one-dimensional layer of cells interacting via NDJ pathway, for different values of Fringe effect. Our results show that at high Fringe effect, the tissue level pattern of similar fates is disrupted and the ‘salt-and-pepper’ pattern starts to emerge (figure 5). Our results are consistent with experiments suggesting that Fringe promotes lateral inhibition during neurogenesis [51].

#### Fringe alters the relative stability of the steady states of NDJ signaling

In order to evaluate the effect of noise in the NDJ circuit for two-cell system, we represent the phase space by an effective potential for different values of Fringe effect. The effective potential depends on the levels of Notch of each cell, and is defined as  $U = -\log(P)$ , where  $P = P(N_1, N_2)$  is the probability density at the two dimensional phase space ( $N_1 \times N_2$ ) which is calculated by using the Euler–Maruyama method to approximate the ordinary

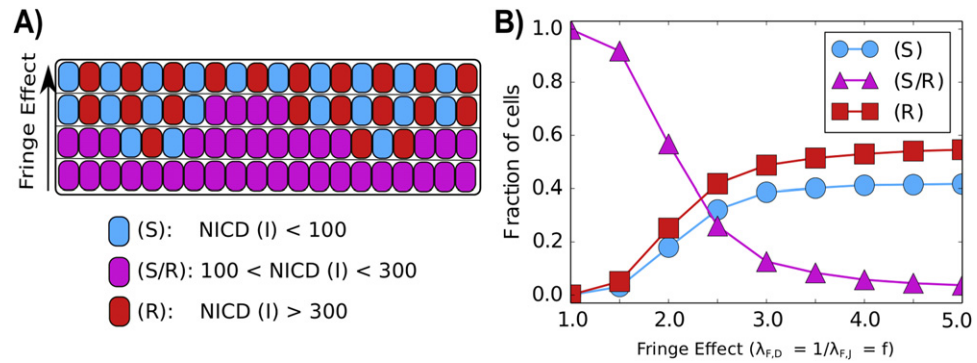


**Figure 5.** Fringe effect on tissue-level patterning. (A) Representation of a one-dimensional layer of cells interacting through Notch signaling for different levels of Fringe effect. (B) The average of the fraction of cells in (S), (S/R) or (R) state as a function of the effect of Fringe. Increase in Fringe effect promotes lateral inhibition—formation of ‘salt and pepper’ alternate patterns of cell fate in adjacent cells. The averages were taken over 100 simulations of a one-dimensional layer of 100 interacting cells with periodic boundary condition. The steady states (S, R and S/R) are defined in terms of the level of NICD ( $I$ ). If  $I$  is close to the Hill function threshold of NICD ( $I_0 = 200$  molecules, see discussion in SI section S1) the cell is in the S/R state, if  $I$  is much higher than  $I_0$ , the cell is a Receiver and if  $I$  is much lower than  $I_0$ , the cell is a Sender. Therefore: (S:  $I < 100$ , S/R:  $100 < I < 300$ , R:  $I > 300$ ).

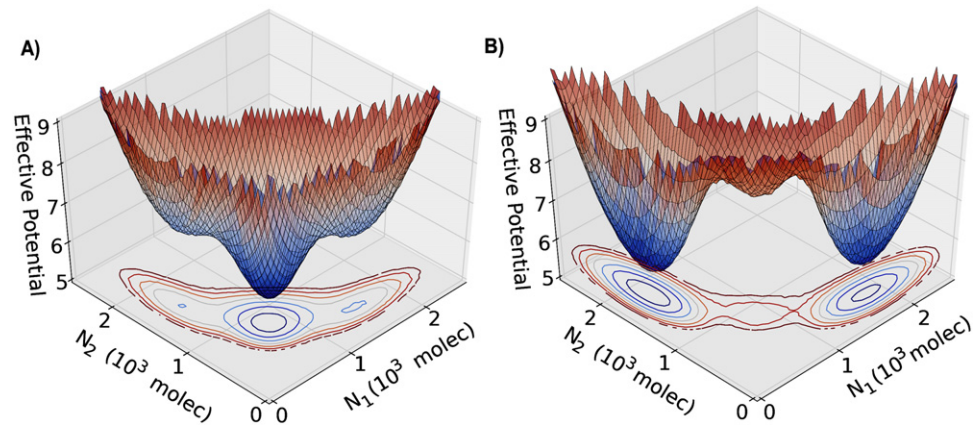
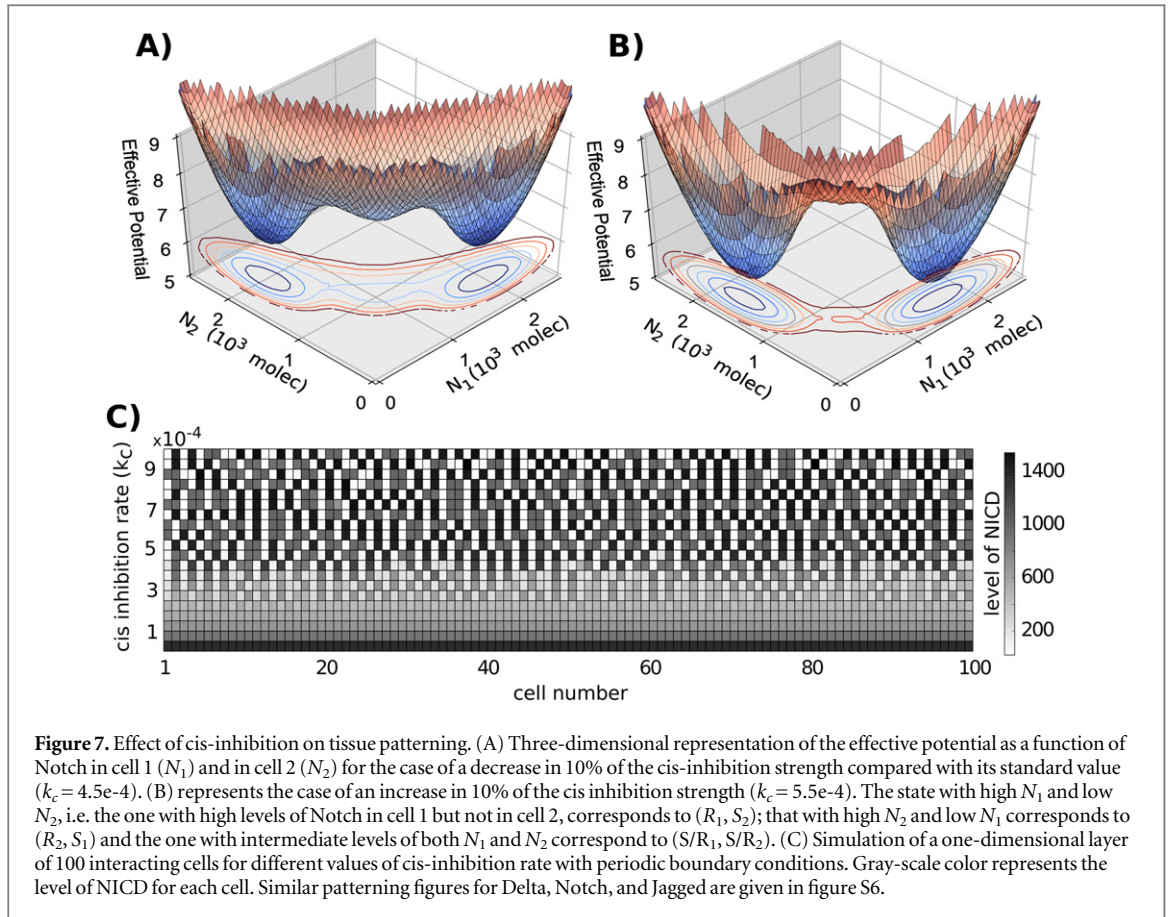


**Figure 6.** Three-dimensional representation of the effective potential as a function of Notch in cell 1 ( $N_1$ ) and in cell 2 ( $N_2$ ). The effective potential is defined as  $U = -\log(P)$ , where  $P = P(N_1, N_2)$  is the probability density calculated by solving the differential equations stochastically using the Euler–Maruyama method. (A) represents the case of no effect of Fringe ( $f = 1.0$ ). (B) represents the case considering the effect of Fringe ( $f = 1.5$ ). The state with high  $N_1$  and low  $N_2$ , i.e. the one with high levels of Notch in cell 1 but not in cell 2, corresponds to  $(R_1, S_2)$ ; that with high  $N_2$  and low  $N_1$  corresponds to  $(R_2, S_1)$  and the one with intermediate levels of both  $N_1$  and  $N_2$  correspond to  $(S/R_1, S/R_2)$ .

differential equation to a stochastic differential equation [52]. We observed three states of the system: (i) first cell behaves as a Sender (low Notch) and the second one as a Receiver (high Notch)— $(S_1, R_2)$ , (ii) first cell behaves as a Receiver (high Notch) and the second one as a Sender (low Notch)— $(R_1, S_2)$ , and (iii) both cells behave as both Sender and Receiver (both with intermediate level of Notch)— $(S/R_1, S/R_2)$ . For low or no effect of Fringe, both the cells tend to stay predominantly in the hybrid S/R state— $(S/R_1, S/R_2)$  and alternate their fates only sporadically (figure 6(A)). However, when the Fringe effect is strong, the basin of attraction of the  $(S/R_1, S/R_2)$  state becomes shallower and therefore small fluctuations can move the cells to one of the two states that now have a deep basin of attraction; thus one cell starts behaving as a Receiver (R; high Notch), and the other as a Sender (S; low Notch)— $(S_1, R_2)$  or  $(R_1, S_2)$  (figure 6(B)).

These results indicate that Fringe promotes lateral inhibition by stabilizing alternate Sender and Receiver fates between neighboring cells. Thus, loss of Fringe is expected to stabilize the hybrid S/R state, i.e. the outcome of NJ signaling. Because NJ signaling is more often implicated than ND signaling in many aspects of tumor progression [19], our results on the role of Fringe in the inhibition of NJ signaling rationalize the fact that Fringe has been reported as a tumor suppressor in multiple cancers such as prostate, lung and basal-like breast cancer (BLBC) [53–55]. Further, loss of Fringe facilitates NJ signaling that is critical in the tumorigenesis of BLBCs [53].

In mammals, Fringe can have three homologues—Lunatic Fringe (Lfng), Manic Fringe (Mfng) and Radical Fringe (Rfng). It should be noted that the results about Fringe promoting ND signaling and lateral inhibition



hold true for those homologues that have similar circuit architecture with Notch signaling as considered here, i.e. they promote ND signaling both in *cis* and in *trans*, and they are activated by NICD. Among the existing homologues, only *Lfng* has been shown to be a direct downstream target of NICD [13]; and both *Lfng* and *Mfng*, but not *Rfng*, promotes ND signaling [14]. Consistently, both *Lfng* and *Mfng*, but not *Rfng*, has been reported to be a tumor suppressor [53–55]. Future models should consider the effect of these different Fringe homologues distinctly.

### Cis-inhibition facilitates lateral inhibition patterning

*Cis*-inhibition, i.e. cell-autonomous binding and consequent degradation of the receptor and ligand, has been reported to be critical for lateral inhibition and pattern formation in multiple developmental contexts such as sensory organ precursors and *Drosophila* wing primordium [56–58], but it is not present in other contexts such as hair cell formation in the inner ear [59]. Furthermore, the role of cis-inhibition in angiogenesis remains enigmatic [48].

To decipher the role of *cis*-inhibition in lateral inhibition patterning, we evaluate its effect on the stability of cell-fate decisions, and represent the phase space by an effective potential for the case of both lower and higher *cis*-inhibition rate ( $k_c$ ). At higher  $k_c$ , the basin of attraction for the  $(S/R_1, S/R_2)$  becomes shallow and those for the  $(S_1, R_2)$  and  $(R_1, S_2)$  become deeper, i.e. at higher levels of cis-inhibition, adjacent cells are much more likely to adopt alternate fates of one being the sender and the other receiver than similar fates of being hybrid S/R ones (figures 7(A) and (B)). These results for the role of *cis*-inhibition in NDJ signaling are consistent with previous observations about *cis*-inhibition in ND signaling that it can facilitate pattern formation even without any cooperativity in ND interaction, and usually confers faster dynamics and greater robustness to noise during patterning [26, 41, 56].

Next, we evaluate the effect of *cis*-inhibition in tissue patterning. Increased *cis*-inhibition facilitates ‘salt-and-pepper’ or alternate Sender and Receiver patterning, whereas decreased *cis*-inhibition leads the cells to attain the same fate of hybrid S/R (figure 7(C)). Interestingly, the hybrid S/R state observed at lower *cis*-inhibition has very high levels of NICD (as compared to levels of NICD in other simulations in our analysis), Notch and Jagged, but low levels of Delta (figure 7(C), figure S6), thereby suggesting that *cis*-inhibition can maintain low levels of NICD and Notch in a cell-autonomous manner. Our results are corroborated by experiments showing that *cis*-inhibition can act as a buffer for cells against accidental Notch activity [60]. This proposed novel role of *cis*-

inhibition is also indicative of its ability to attenuate NJ signaling similar to Fringe, and therefore *cis*-inhibition might as well act as a tumor suppressor.

Such insights into pattern formation are a direct outcome of coordinated cell-fate decisions happening at sub-cellular level, and can be gained only after analyzing a multi-cell model of NDJ signaling, as presented here. Results about relative stability of signaling states for one cell have implications about the spatiotemporal stability of tissue-level patterns. By considering multiple types of cells with different signaling modalities among themselves in a theoretical model, the pattern formation dynamics at a tissue level can give way to organ level dynamics, hence linking ‘network biology’ to ‘network physiology’ [1, 2]. Further, as shown recently, ND signaling can happen without cell–cell contact as well—through exosomes (cell-derived vesicles that can play a key role in long-range cell–cell communication) [61]. These exosomes, that can circulate in blood to reach other organs as well as be released by both tumor and stroma cells for targeted interaction [62], might constitute a key component of vertical integration from sub-cellular level to organ level both during development and disease.

### Soluble ligands affect cell-fate decision in a paracrine manner

In addition to transmembrane ligands, Notch signaling can also be activated by binding of Notch receptor to soluble ligands that can be secreted by other cells [23, 29]. Transmembrane ligands activate Notch signaling and hence affect cell-fate decisions in a juxtacrine (cell–cell contact) manner, but soluble ligands function through paracrine (one cell secretes a ligand that can bind to nearby cells and induce a response) manner, thereby sometimes competing for the available Notch receptors on the surface [63]. However, the soluble ligands usually activate Notch weakly, i.e. have a lower *trans*-activation rate for Notch [32].

To evaluate the role of soluble ligand-mediated paracrine signaling in cell-fate decision making, we incorporated the soluble forms of ligands Delta and Jagged in our two-cell system (two identical cells communicating via NDJ pathway), as described in equations (11)–(14) where  $D_{\text{ext}}$  and  $J_{\text{ext}}$  represents Delta and Jagged of the neighboring cell and  $D_{\text{ext}}^s$  and  $J_{\text{ext}}^s$  represent soluble Delta and Jagged respectively. Here, the soluble ligands have been incorporated in the model so as to mimic the biological situation where tumor cells are exposed to soluble Jagged from stromal cells, i.e. soluble ligands are only produced by stroma, and not tumor cells themselves that still interact via transmembrane ligands only [23]. Thus, levels of soluble ligands have been considered as a parameter and not a dynamic variable of the model.

For the case of paracrine communication via soluble Delta, both the cells tend to behave as Receiver ( $R_1, R_2$ ) for low production rate of Jagged ( $J_0$ ) or both of them behave as hybrid S/R ( $S/R_1, S/R_2$ ) for high  $J_0$ . These cells can adopt opposite fates to each other only for intermediate levels of  $J_0$  and high production rate of Delta ( $D_0$ ) (figures 8(A) and (C), compare with figure 4(A)). Conversely, when the cells interact with soluble Jagged, the cells tend to attain similar fates—hybrid S/R ( $S/R_1, S/R_2$ )—unless the production rate of Delta ( $D_0$ ) is high. For high  $D_0$ , these cells attain opposite fates— one behave as Sender, and the other Receiver ( $S_1, R_2$ ) (figures 8(B) and (D)). Collectively, our results suggest that the soluble ligands—both Delta and Jagged—increase the range of parameters for which both cells attain same fate.

Our results also offer an explanation into why stromal cells secrete Jagged1 more often than Delta [23]. Higher levels of soluble Jagged can enable many cells to adopt a hybrid S/R state (figures 8(B) and (D)), thereby enabling a both-way communication between cancer cells and/or between cancer and stromal cells. Not surprisingly, soluble Delta has been implicated in tumor suppression [64], but soluble Jagged1 facilitates cancer cell survival [65] as well as mediates communication between cancer cells and endothelial cells that leads to increased population of therapy-resistant tumor-initiating CSCs [23].

## Discussion

### The crucial role of hybrid S/R state in tumor progression

Being the key cell–cell communication pathway, Notch signaling circuit also couples to other aspects of cell-fate decision. Two of those modules play a crucial role in cancer metastasis—EMT module and stemness module (figure 9(A)). EMT allows cancer cells to initiate metastasis and travel to different organs in the body, and gaining stemness allows them to initiate a new tumor at those different organs. Here, we discuss the crucial role of hybrid S/R state (that allows bidirectional communication between cancer cells and/or between cancer–stroma) in tumor progression.

#### *Hybrid S/R state allows cancer cells to move and circulate collectively*

EMT is an embryonic program that is aberrantly activated by cancer cells to invade adjacent tissues and gain access to the blood vessels to initiate metastasis. Cells undergoing EMT shed their epithelial traits (cell–cell adhesion, apico-basal polarity, no motility) and gain mesenchymal traits (no cell–cell adhesion, front–back polarity, and individual motility). However, when cells exit the circulation to start a new tumor at a distant

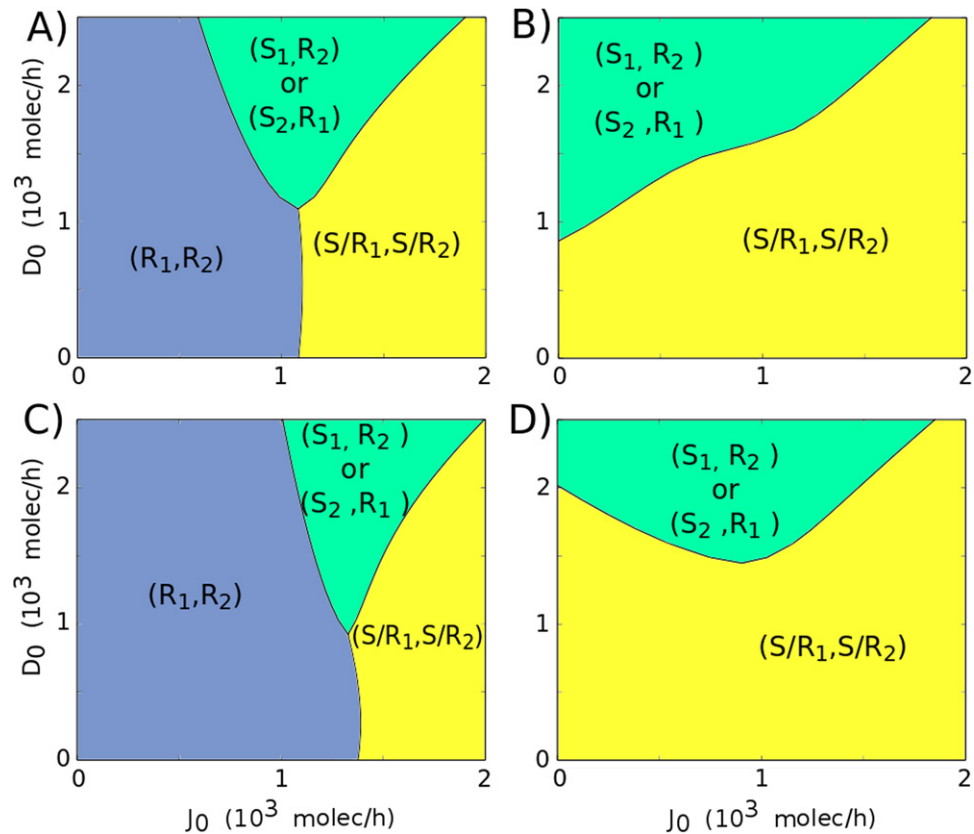


**Figure 8.** Phenotype diagram for two-cell system (two cells interacting via NDJ circuit) when the circuit is driven by the production rates of Jagged ( $J_0$ ) and Delta ( $D_0$ ). Each phase is represented by a different color and corresponds to a different combination of co-existing states. Each diagram represents different levels of soluble ligands Delta ( $D_{ext}^s$ ) and Jagged ( $J_{ext}^s$ ) interacting with these identical cells. (A)  $D_{ext}^s = 600$  molecules,  $J_{ext}^s = 0$ . (B)  $J_{ext}^s = 600$  molecules,  $D_{ext}^s = 0$ . (C)  $D_{ext}^s = 1200$  molecules,  $J_{ext}^s = 0$ . (D)  $J_{ext}^s = 1200$  molecules,  $D_{ext}^s = 0$ . The trans-activation rate for soluble ligands is considered to be three times lower than for membrane-bound ligands ( $k_T^s = k_T/3$ ). The steady states (S, R and S/R) are defined in terms of the level of NICD ( $I$ ). If  $I$  is close to the Hill function threshold of NICD ( $I_0 = 200$  molecules, see discussion in SI section S1) the cell is in the S/R state, if  $I$  is much higher than  $I_0$ , the cell is a Receiver and if  $I$  is much lower than  $I_0$ , the cell is a Sender. Therefore: (S:  $I < 100$ , S/R:  $100 < I < 300$ , R:  $I > 300$ ).

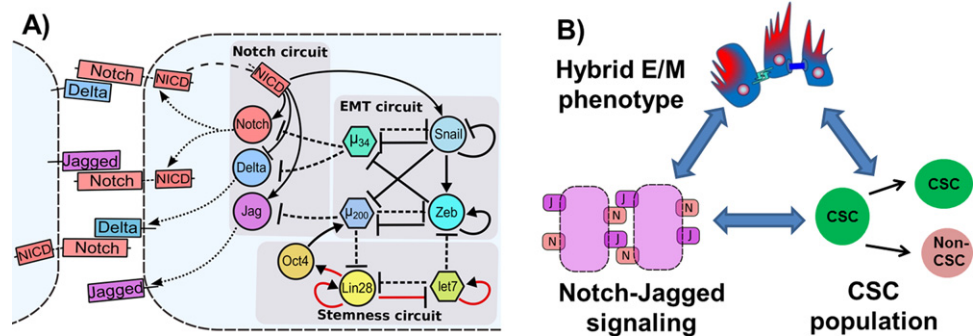


**Figure 9.** Connections between Notch signaling pathway, EMT decision circuit and stemness circuit; and the emergent implications in tumor progression. (A) Notch signaling pathway couples to EMT circuit (miR-200/ZEB and miR-34/SNAIL) in multiple ways—miR-34 inhibits Delta and Notch, and miR-200 inhibits Jagged, and NICD transcriptionally activates Snail. EMT and stemness circuits (LIN28/let-7) also couple with each other—let-7 inhibits ZEB, miR-200 inhibits LIN28, and LIN28 activates miR-200 through OCT4. (see [5, 27, 47] and references therein). Dashed lines represent miR-mediated translational repression, and solid lines represent transcriptional regulation—bars for repression, and arrows for activation. Red arrows represent non-transcriptional regulation. (B) Proposed interconnections between the hybrid E/M phenotype, NJ signaling and maintenance and/or expansion of CSC population. Cell fate convergence achieved via NJ signaling can stabilize the ‘metastable’ hybrid E/M phenotype that is associated with maximum stemness. Also, NJ signaling can maintain and/or expand the CSC population in a non-cell autonomous manner. Filled green circles represent CSCs, and the other filled circle represents non-CSCs (see [22]).

organ, they undergo the reverse of EMT, i.e. Mesenchymal to Epithelial Transition (MET)—to shed their migratory traits and start proliferating to grow secondary tumors or colonize [66]. EMT is a two-step process in which epithelial cells first undergo partial EMT and then complete EMT to become mesenchymal. These two steps in decision-making are mediated by a three-way decision-making switch—a double negative feedback loop between miRNA miR-200 and transcription factor ZEB. The (miR-200/ZEB) circuit allows the cells to attain three phenotypes—epithelial (E—high miR-200, low ZEB), mesenchymal (M—low miR-200, high ZEB) and partial EMT or hybrid epithelial/mesenchymal (E/M—medium miR-200, medium ZEB) [5, 27].

Cells in the hybrid E/M or partial EMT phenotype have mixed epithelial (cell–cell adhesion) and mesenchymal (migration) traits, thereby allowing them to migrate collectively, as observed during wound healing and branching mammary morphogenesis. Such collective migration allows a sheet of cells to migrate by utilizing mechanical forces, and not every individual cell needs to detect and respond to the migration-inducing signal [67–69]. Notch signaling is instrumental during wound healing [70], but if these cells were to communicate mostly via ND, they would have diverse fates from each other (one acts as Sender, and the other Receiver) that can possibly impair wound healing; thus, NJ signaling might help maintain similar fates (hybrid S/R) and hence better co-operation among the cells during wound healing. Therefore, the hybrid S/R state facilitates cell–cell cooperation among collectively migrating cells and may play a crucial role in stabilizing the hybrid E/M phenotype that is otherwise considered to be ‘metastable’ [67].

Recent studies show that cancer hijacks the advantages of collective cell migration from wound healing. During metastasis, the hybrid E/M phenotype is manifested as clusters of CTCs. These clusters can be more resistant to apoptosis in blood circulation, as well as up to 50-times more metastatic than individually migrating cells [71, 72], hence posing a much higher metastatic risk than individually migrating CTCs (a manifestation of the complete EMT phenotype). Further, maintaining the partial EMT phenotype might confer higher plasticity to cells to adapt to the changing microenvironment that can be useful for cells to revert to an epithelial phenotype during colonization, as well as continuing subsequent rounds of metastasis [73]. We hypothesize that Notch signaling pathway is critical in maintaining the clusters of CTCs together and therefore targeting it can have important possible therapeutic applications.

To test this hypothesis, future modeling attempts should incorporate the molecular links known between EMT and Notch signaling—miR-200 and miR-34, miRNAs that restrict EMT, can inhibit the translation of Delta, Jagged and Notch [74–77]. Further, Notch signaling can induce EMT by activating the transcription factor SNAIL [78, 79] that inhibits miR-200 (figure 9(A)) and is required for cell survival during partial EMT and facilitates ‘re-epithelialization’ of hybrid E/M cells [80, 81].

Activation of EMT in cancer cells also leads to an increase in their tumor-initiating capabilities or transform them to being like CSCs—the therapy-resistant cancer cells that act as a reservoir for new, more differentiated tumor cells, as well as maintain the ability to self-renew for many generations, thereby initiating a tumor [82, 83]. Recent studies show that cells undergoing partial EMT can gain ‘stemness’ that can be compromised significantly if cells undergo complete EMT and become mesenchymal-like [47, 84–87]; thereby highlighting another advantage of collectively migrating CTCs during metastatic progression. All these functional advantages of collective cell migration or hybrid E/M phenotype—resistance to cell death during circulation, higher plasticity to both colonize and reinitiate metastasis, and enhanced tumor-initiating abilities—might be attained only in the presence of the cell–cell communication based stabilizing interactions provided by NDJ signaling (figure 9(B)).

#### *Hybrid S/R state increases CSC population*

In addition to links through the EMT module, Notch signaling and CSCs or cells with tumor-initiating abilities are interconnected in multiple ways. Notch and Jagged, but not Delta, are overexpressed in CSCs as compared to non-CSCs in multiple cancers—glioblastoma, pancreatic cancer as well as BLBC [22, 88–90]. This overexpression of Notch and Jagged can potentially explain the role of Notch signaling in mediating therapy resistance [90–92]. It may be noted that CSCs only form a small percentage of total cancer cells, but the way they divide can affect tumor progression drastically—(i) if a CSCs divides to form two non-CSCs, that can lead to depletion of CSC pool; (ii) if a CSC divides to give rise to one CSC and one non-CSC, that can maintain the CSC population; and (iii) if a CSC divides to give rise to both CSCs, that can expand the CSC population. A recent study suggests that Notch/miR-34 axis decides the mechanism of cell division of CSCs—high miR-34 levels lead to low Notch levels and differentiation of CSC to non-CSCs, low miR-34 levels lead to high Notch levels and division of one CSC to two CSCs, and consequently medium miR-34 levels lead to medium Notch levels and hence asymmetric cell division of CSCs [75]. Therefore, activation of Notch signaling, to medium or high levels, can maintain or expand the CSC pool respectively.

Another absolutely critical player that mediates the connection between Notch and CSCs is inflammation. The inflammatory cytokines such as TNF- $\alpha$  and IL-6 can both increase CSC population as well as increase the production rate of Jagged [48, 93]. Recent studies indicate that the increase in CSC population is mediated by

high levels of Jagged. Further, Jagged is also secreted by many stromal cells [23], thus the NJ signaling might be more frequently activated in tumor microenvironment than the ND one. Higher levels of soluble Jagged, but not soluble Delta, can enable a population of cells to adopt a hybrid S/R state (figures 8(B) and (D)) that facilitates bidirectional communication between cancer cells and/or between cancer and stroma, thereby offering a possible explanation of why stromal cells often secrete soluble Jagged, but not Delta. As noted earlier, higher levels of Notch and Jagged can also expand the population of therapy-resistant and tumor-initiating CSCs [22, 23, 94, 95].

Future modeling studies should explore the interplay between Notch, inflammation and asymmetric versus symmetric cell division of CSCs in a cell-population model. Many models have explored the effect of CSCs on tumor progression in terms of population dynamics, but without considering any cell–cell communication [96–99]. Since cell–cell communication is fundamental during collective decision-making of many populations, an understanding of tumor progression without considering cell–cell interaction via NDJ signaling is incomplete, and hence cannot be utilized to plan an effective and strategic ‘cyber war’ against them [100].

## Conclusion

NDJ signaling behaves as a three-way switch, allowing the cell three states—Sender (S—high ligand, low receptor), Receiver (R—low ligand, high receptor) and hybrid S/R(S/R—medium ligand, medium receptor). We elucidate the operating principles of a system of two cells interacting via NDJ signaling. High production rate of Jagged and high levels of soluble Jagged expands the range of parameters under which both these cells attain the hybrid S/R state. Conversely, high levels of Delta, Fringe and cis-inhibition between Notch and either of its ligands reduce this range of conditions, thereby promoting cell-fate divergence. We also discuss the fundamental role of hybrid S/R state in promoting cancer metastasis by enabling collective cell migration and expanding the CSC population.

## Acknowledgments

We have benefited from discussions with Professor Herbert Levine. This work was supported by the National Science Foundation (NSF) (Grants PHY-1427654 and MCB-1214457) and by the Cancer Prevention and Research Institute of Texas (CPRIT). MB was also supported by FAPESP Grant 2013/14438-8. JNO is a CPRIT Scholar in Cancer Research sponsored by the Cancer Prevention and Research Institute of Texas. CC was also supported by NSF Grants CHE 1265929 and 1152344 and Welch foundation Grant C1570. EB-J was also supported by a grant from the Tauber Family Funds and the Maguy-Glass Chair in Physics of Complex Systems. ML was also supported by a training fellowship from Keck Center for Interdisciplinary Bioscience Training of the Gulf Coast Consortia CPRIT Grant RP140113.

## References

- [1] Bashan A, Bartsch R P, Kantelhardt J W, Havlin S and Ivanov P C 2012 Network physiology reveals relations between network topology and physiological function *Nat. Commun.* **3** 702
- [2] Ivanov P C and Bartsch R P 2014 Network physiology: mapping interactions between networks of physiologic networks *Networks of Networks: the last Frontier of Complexity* ed G D’Agostino and A Scala (Switzerland: Springer) pp 203–22
- [3] Lewis J 2008 From signals to patterns: space, time, and mathematics in developmental biology *Science* **322** 399–403
- [4] Balázsi G, van Oudenaarden A and Collins J J 2011 Cellular decision making and biological noise: from microbes to mammals *Cell* **144** 910–25
- [5] Lu M, Jolly M K, Onuchic J and Ben-Jacob E 2014 Toward decoding the principles of cancer metastasis circuits *Cancer Res.* **74** 4574–87
- [6] Ben-Jacob E, Lu M, Schultz D and Onuchic J N 2014 The physics of bacterial decision making *Front. Cell. Infect. Microbiol.* **4** 154
- [7] Andersson E R, Sandberg R and Lendahl U 2011 Notch signaling: simplicity in design, versatility in function *Development* **138** 3593–612
- [8] Shaya O and Sprinzak D 2011 From Notch signaling to fine-grained patterning: modeling meets experiments *Curr. Opin. Genet. Dev.* **21** 732–9
- [9] Timmerman L A et al 2004 Notch promotes epithelial-mesenchymal transition during cardiac development and oncogenic transformation *Genes Dev.* **18** 99–115
- [10] Petrovic J, Formosa-Jordan P, Luna-Escalante J C, Abelló G, Ibañes M, Neves J and Giraldez F 2014 Ligand-dependent Notch signaling strength orchestrates lateral induction and lateral inhibition in the developing inner ear *Development* **141** 2313–24
- [11] Manderfield L J, High F A, Engleka K A, Liu F, Li L, Rentschler S and Epstein J A 2012 Notch activation of Jagged1 contributes to the assembly of the arterial wall *Circulation* **125** 314–23
- [12] Hartman B H, Reh T A and Bermingham-McDonogh O 2010 Notch signaling specifies prosensory domains via lateral induction in the developing mammalian inner ear *Proc. Natl Acad. Sci. USA* **107** 15792–7
- [13] Morales A V, Yasuda Y and Ish-horowicz D 2002 Periodic lunatic fringe expression is controlled during segmentation by a cyclic transcriptional enhancer responsive to Notch signaling *Dev. Cell* **3** 63–74

- [14] LeBon L, Lee T V, Sprinzak D, Jafar-Nejad H and Elowitz M B 2014 Fringe proteins modulate Notch–ligand cis and trans interactions to specify signaling states *eLife* **3** e02950
- [15] Panin V M, Papayannopoulos V, Wilson R and Irvine K D 1997 Fringe modulates Notch–ligand interactions *Nature* **387** 908–12
- [16] Hicks C, Johnston S H, diSibio G, Collazo A, Vogt T F and Weinmaster G 2000 Fringe differentially modulates Jagged1 and Delta1 signalling through Notch1 and Notch2 *Nat. Cell Biol.* **2** 515–20
- [17] Shimizu K, Chiba S, Saito T, Kumano K, Takahashi T and Hirai H 2001 Manic fringe and lunatic fringe modify different sites of the Notch2 extracellular region, resulting in different signaling modulation *J. Biol. Chem.* **276** 25753–8
- [18] Van De Walle et al 2011 Jagged2 acts as a Delta-like Notch ligand during early hematopoietic cell fate decisions *Blood* **117** 4449–59
- [19] Li D, Masiero M, Banham A H and Harris A L 2014 The notch ligand JAGGED1 as a target for anti-tumor therapy *Front. Oncol.* **4** 254
- [20] Sethi N, Dai X, Winter C G and Kang Y 2011 Tumor-derived JAGGED1 promotes osteolytic bone metastasis of breast cancer by engaging notch signaling in bone cells *Cancer Cell* **19** 192–205
- [21] Gupta G P and Massagué J 2006 Cancer metastasis: building a framework *Cell* **127** 679–95
- [22] Yamamoto M, Taguchi Y, Ito-Kureha T, Semba K, Yamaguchi N and Inoue J 2013 NF- $\kappa$ B non-cell-autonomously regulates cancer stem cell populations in the basal-like breast cancer subtype *Nat. Commun.* **4** 2299
- [23] Lu J et al 2013 Endothelial cells promote the colorectal cancer stem cell phenotype through a soluble form of Jagged-1 *Cancer Cell* **23** 171–85
- [24] Ghiabi P, Jiang J, Pasquier J, Maleki M, Abu-Kaoud N, Rafii S and Rafii A 2014 Endothelial cells provide a notch-dependent pro-tumoral niche for enhancing breast cancer survival, stemness and pro-metastatic properties *PLoS One* **9** e112424
- [25] Boareto M, Jolly M K, Lu M, Onuchic J N, Clementi C and Ben-Jacob E 2015 Jagged–Delta asymmetry in Notch signaling can give rise to a Sender/Receiver hybrid phenotype *Proc. Natl Acad. Sci.* **112** E402–9
- [26] Sprinzak D, Lakhnpal A, Lebon L, Santat L A, Fontes M E, Anderson G A, Garcia-Ojalvo J and Elowitz M B 2010 Cis-interactions between Notch and Delta generate mutually exclusive signalling states *Nature* **465** 86–90
- [27] Lu M, Jolly M K, Levine H, Onuchic J N and Ben-Jacob E 2013 MicroRNA-based regulation of epithelial-hybrid-mesenchymal fate determination *Proc. Natl Acad. Sci. USA* **110** 18174–9
- [28] Wang M M 2011 Notch signaling and Notch signaling modifiers *Int. J. Biochem. Cell Biol.* **43** 1550–62
- [29] Urs S, Roudabush A, O'Neill C F, Pinz I, Prudovsky I, Kacer D, Tang Y, Liaw L and Small D 2008 Soluble forms of the Notch ligands Delta1 and Jagged1 promote *in vivo* tumorigenicity in NIH3T3 fibroblasts with distinct phenotypes *Am. J. Pathol.* **173** 865–78
- [30] Musse A A, Meloty-Kapella L and Weinmaster G 2012 Notch ligand endocytosis: mechanistic basis of signaling activity *Semin. Cell Dev. Biol.* **23** 429–36
- [31] Hicks C, Ladi E, Lindsell C, Hsieh J J D, Hayward S D, Collazo A and Weinmaster G 2002 A secreted Delta1-Fc fusion protein functions both as an activator and inhibitor of Notch1 signaling *J. Neurosci. Res.* **68** 655–67
- [32] Narui Y and Salaita K 2013 Membrane tethered Delta activates Notch and reveals a role for spatio-mechanical regulation of the signaling pathway *Biophys. J.* **105** 2655–65
- [33] Clewley R 2012 Hybrid models and biological model reduction with PyDSTool *PLoS Comput. Biol.* **8** e1002628
- [34] Wilkinson H A, Fitzgerald K and Greenwald I 1994 Reciprocal changes in expression of the receptor lin-12 and its ligand lag-2 prior to commitment in a *C. elegans* cell fate decision *Cell* **79** 1187–98
- [35] Collier J R, Monk N A, Maini P K and Lewis J H 1996 Pattern formation by lateral inhibition with feedback: a mathematical model of delta–notch intercellular signalling *J. Theor. Biol.* **183** 429–46
- [36] Jakobsson L et al 2010 Endothelial cells dynamically compete for the tip cell position during angiogenic sprouting *Nat. Cell Biol.* **12** 943–53
- [37] Formosa-Jordan P, Ibañes M, Ares S and Frade J-M 2013 Lateral inhibition and neurogenesis: novel aspects in motion *Int. J. Dev. Biol.* **57** 341–50
- [38] Chen J S, Gumbayan A M, Zeller R W and Mahaffy J M 2014 An expanded Notch–Delta model exhibiting long-range patterning and incorporating MicroRNA regulation *PLoS Comput. Biol.* **10** e1003655
- [39] Owen M R, Sherratt J A and Wearing H J 2000 Lateral induction by juxtacrine signaling is a new mechanism for pattern formation *Dev. Biol.* **217** 54–61
- [40] de Back W, Zhou J X and Brusch L 2013 On the role of lateral stabilization during early patterning in the pancreas *J. R. Soc. Interface* **10** 20120766
- [41] Sprinzak D, Lakhnpal A, LeBon L, Garcia-Ojalvo J and Elowitz M B 2011 Mutual inactivation of Notch receptors and ligands facilitates developmental patterning *PLoS Comput. Biol.* **7** e1002069
- [42] Formosa-Jordan P and Ibañes M 2014 Competition in Notch signaling with Cis enriches cell fate decisions *PLoS One* **9** e95744
- [43] Lu M, Jolly M K, Gomoto R, Huang B, Onuchic J and Ben-Jacob E 2013 Tristability in cancer-associated MicroRNA-TF chimera toggle switch *J. Phys. Chem. B* **117** 13164–74
- [44] Huang B, Lu M, Jolly M K, Tsarfaty I, Onuchic J and Ben-Jacob E 2014 The three-way switch operation of Rac1/RhoA GTPase-based circuit controlling amoeboid-hybrid-mesenchymal transition *Sci. Rep.* **4** 6449
- [45] Andrecut M, Halley J D, Winkler D A and Huang S 2011 A general model for binary cell fate decision gene circuits with degeneracy: indeterminacy and switch behavior in the absence of cooperativity *PLoS One* **6** e19358
- [46] Macia J, Widder S and Solé R 2009 Why are cellular switches boolean? General conditions for multistable genetic circuits *J. Theor. Biol.* **261** 126–35
- [47] Jolly M K, Huang B, Lu M, Mani S A, Levine H and Ben-Jacob E 2014 Towards elucidating the connection between epithelial-mesenchymal transitions and stemness *J. R. Soc. Interface* **11** 20140962
- [48] Benedetto R, Roca C, Sørensen I, Adams S, Gossler A, Fruttiger M and Adams R H 2009 The Notch ligands Dll4 and Jagged1 have opposing effects on angiogenesis *Cell* **137** 1124–35
- [49] Benedetto R and Hellström M 2013 Notch as a hub for signaling in angiogenesis *Exp. Cell Res.* **319** 1281–8
- [50] De Back W, Zimm R and Brusch L 2013 Transdifferentiation of pancreatic cells by loss of contact-mediated signaling *BMC Syst. Biol.* **7** 77
- [51] Nikolaou N, Watanabe-Asaka T, Gerety S, Distel M, Köster R W and Wilkinson D G 2009 Lunatic fringe promotes the lateral inhibition of neurogenesis *Development* **136** 2523–33
- [52] Lu M, Onuchic J and Ben-Jacob E 2014 Construction of an Effective Landscape for Multistate Genetic Switches *Phys. Rev. Lett.* **113** 078102
- [53] Xu K et al 2012 Lunatic fringe deficiency cooperates with the met/caveolin gene amplicon to induce basal-like breast cancer *Cancer Cell* **21** 626–41

- [54] Yi F, Amarasinghe B and Dang T P 2013 Manic fringe inhibits tumor growth by suppressing Notch3 degradation in lung cancer *Am. J. Cancer Res.* **3** 490–9
- [55] Zhang S, Chung W, Wu G, Egan S E and Xu K 2014 Tumor-suppressive activity of lunatic fringe in prostate through differential modulation of Notch receptor activation *Neoplasia* **16** 158–67
- [56] Barad O, Rosin D, Hornstein E and Barkai N 2010 Error minimization in lateral inhibition circuits *Sci. Signal* **3** ra51
- [57] Becam I, Fiuza U-M, Arias A M and Milán M 2010 A role of receptor Notch in ligand cis-inhibition in *Drosophila* *Curr. Biol.* **20** 554–60
- [58] Miller A C, Lyons E L and Herman T G 2009 Cis-inhibition of Notch by endogenous Delta biases the outcome of lateral inhibition *Curr. Biol.* **19** 1378–83
- [59] Chrysostomou E, Gale J E and Daudet N 2012 Delta-like 1 and lateral inhibition during hair cell formation in the chicken inner ear: evidence against cis-inhibition *Development* **139** 3764–74
- [60] Palmer W H, Jia D and Deng W-M 2015 Cis-interactions between Notch and its ligands block ligand-independent Notch activity *eLife* **3** e04415
- [61] Sheldon H et al 2010 New mechanism for Notch signaling to endothelium at a distance by Delta-like 4 incorporation into exosomes *Blood* **116** 2385–94
- [62] Lu M, Huang B, Hanash S M, Onuchic J N and Ben-Jacob E 2014 Modeling putative therapeutic implications of exosome exchange between tumor and immune cells *Proc. Natl Acad. Sci. USA* **111** E4165–74
- [63] D'Souza B, Miyamoto A and Weinmaster G 2008 The many facets of Notch ligands *Oncogene* **27** 5148–67
- [64] Li J-L et al 2007 Delta-like 4 Notch ligand regulates tumor angiogenesis, improves tumor vascular function, and promotes tumor growth *in vivo* *Cancer Res.* **67** 11244–53
- [65] Rosati E, Sabatini R, Rampino G, Tabilio A, Di Ianni M, Fettucciari K, Bartoli A, Coaccioli S, Screpanti I and Marconi P 2009 Constitutively activated Notch signaling is involved in survival and apoptosis resistance of B-CLL cells *Blood* **113** 856–65
- [66] Nieto M A 2013 Epithelial plasticity: a common theme in embryonic and cancer cells. *Science* **342** 1234850
- [67] Arnoux V, Nassour M, Helgoualc A L, Hipskind R A and Savagner P 2008 Erk5 controls Slug expression and keratinocyte activation during wound healing *Mol. Biol. Cell* **19** 4738–49
- [68] Micalizzi D S, Farabaugh S M and Ford H L 2010 Epithelial–mesenchymal transition in cancer: parallels between normal development and tumor progression *J. Mammary Gland Biol. Neoplasia* **15** 117–34
- [69] Revenu C and Gilmour D 2009 EMT 2.0: shaping epithelia through collective migration *Curr. Opin. Genet. Dev.* **19** 338–42
- [70] Chigurupati S et al 2007 Involvement of notch signaling in wound healing *PLoS One* **2** e1167
- [71] Yu M et al 2013 Circulating breast tumor cells exhibit dynamic changes in epithelial and mesenchymal composition *Science* **339** 580–4
- [72] Aceto N et al 2014 Circulating tumor cell clusters are oligoclonal precursors of breast cancer metastasis *Cell* **158** 1110–22
- [73] Bednarz-Knoll N, Alix-Panabières C and Pantel K 2012 Plasticity of disseminating cancer cells in patients with epithelial malignancies *Cancer Metastasis Rev.* **31** 673–87
- [74] Vallejo D M, Caparros E and Dominguez M 2011 Targeting Notch signalling by the conserved miR-8/200 microRNA family in development and cancer cells *EMBO J.* **30** 756–69
- [75] Bu P et al 2013 A microRNA miR-34a-regulated bimodal switch targets notch in colon cancer stem cells *Cell Stem Cell* **12** 602–15
- [76] Pang R T, Leung C O, Ye T M, Liu W, Chiu P C, Lam K K, Lee K F and Yeung W S 2010 MicroRNA-34a suppresses invasion through downregulation of Notch1 and Jagged1 in cervical carcinoma and choriocarcinoma cells *Carcinogenesis* **31** 1037–44
- [77] De Antonellis P et al 2011 MiR-34a targeting of Notch ligand delta-like 1 impairs CD15+/CD133+ tumor-propagating cells and supports neural differentiation in medulloblastoma *PLoS One* **6** e24584
- [78] Sahlgren C, Gustafsson M V, Jin S, Poellinger L and Lendahl U 2008 Notch signaling mediates hypoxia-induced tumor cell migration and invasion *Proc. Natl Acad. Sci. USA* **105** 6392–7
- [79] Niessen K, Fu Y, Chang L, Hoodless P A, McFadden D and Karsan A 2008 Slug is a direct Notch target required for initiation of cardiac cushion cellularization *J. Cell Biol.* **182** 315–25
- [80] Savagner P, Kusewitt D F, Carver E A, Magnino F, Choi C, Gridley T and Hudson L G 2005 Developmental transcription factor slug is required for effective re-epithelialization by adult keratinocytes *J. Cell. Physiol.* **202** 858–66
- [81] Leroy P and Mostov K E 2007 Slug is required for cell survival during partial epithelial-mesenchymal transition of HGF-induced tubulogenesis *Mol. Biol. Cell* **18** 1943–52
- [82] Mani S A et al 2008 The epithelial-mesenchymal transition generates cells with properties of stem cells *Cell* **133** 704–15
- [83] Morel A-P, Lièvre M, Thomas C, Hinkal G, Ansieau S and Puisieux A 2008 Generation of breast cancer stem cells through epithelial-mesenchymal transition *PLoS One* **3** e2888
- [84] Ombrato L and Malanchi I 2014 The EMT universe: space between cancer cell dissemination and metastasis initiation *Crit. Rev. Oncog.* **19** 349–61
- [85] Pattabiraman D R and Weinberg R A 2014 Tackling the cancer stem cells—what challenges do they pose? *Nat. Rev. Drug Discovery* **13** 497–512
- [86] Conigliaro A et al 2013 Evidence for a common progenitor of epithelial and mesenchymal components of the liver *Cell Death Differ.* **20** 1116–23
- [87] Strauss R et al 2011 Analysis of epithelial and mesenchymal markers in ovarian cancer reveals phenotypic heterogeneity and plasticity *PLoS One* **6** e16186
- [88] Sikandar S S, Pate K T, Anderson S, Dizon D, Edwards R A, Waterman M L and Lipkin S M 2010 NOTCH signaling is required for formation and self-renewal of tumor-initiating cells and for repression of secretory cell differentiation in colon cancer *Cancer Res.* **70** 1469–78
- [89] Zhu T S et al 2011 Endothelial cells create a stem cell niche in glioblastoma by providing NOTCH ligands that nurture self-renewal of cancer stem-like cells *Cancer Res.* **71** 6061–72
- [90] Wang Z, Li Y, Kong D, Banerjee S, Ahmad A, Azmi A S, Ali S, Abbruzzese J L, Gallick G E and Sarkar F H 2009 Acquisition of epithelial-mesenchymal transition phenotype of gemcitabine-resistant pancreatic cancer cells is linked with activation of the notch signaling pathway *Cancer Res.* **69** 2400–7
- [91] Kamdje A H N, Bassi G, Pacelli L, Malpeli G, Amati E, Nichele I, Pizzolo G and Krampera R 2012 Role of stromal cell-mediated Notch signaling in CLL resistance to chemotherapy *Blood Cancer J.* **2** e73
- [92] Nefedova Y, Sullivan D M, Bolick S C, Dalton W S and Gabrilovich D I 2008 Inhibition of Notch signaling induces apoptosis of myeloma cells and enhances sensitivity to chemotherapy *Blood* **111** 2220–9
- [93] Iliopoulos D, Hirsch H A, Wang G and Struhl K 2011 Inducible formation of breast cancer stem cells and their dynamic equilibrium with non-stem cancer cells via IL6 secretion *Proc. Natl Acad. Sci. USA* **108** 1397–402

- [94] Lee S H, Hong H S, Liu Z X, Kim R H, Kang M K, Park N-H and Shin K-H 2012 TNF $\alpha$  enhances cancer stem cell-like phenotype via Notch-Hes1 activation in oral squamous cell carcinoma cells *Biochem. Biophys. Res. Commun.* **424** 58–64
- [95] Chang Q *et al* 2013 The IL-6/JAK/Stat3 feed-forward loop drives tumorigenesis and metastasis *Neoplasia* **15** 848–62
- [96] Liu X *et al* 2013 Nonlinear growth kinetics of breast cancer stem cells: implications for cancer stem cell targeted therapy *Sci. Rep.* **3** 2473
- [97] Fornari C, Beccuti M, Lanzardo S, Conti L, Balbo G, Cavallo F, Calogero R A and Cordero F 2014 A mathematical-biological joint effort to investigate the tumor-initiating ability of cancer stem cells *PLoS One* **9** e106193
- [98] Zhou D, Wang Y and Wu B 2014 A multi-phenotypic cancer model with cell plasticity *J. Theor. Biol.* **357** 35–45
- [99] Turner C and Kohandel M 2010 Investigating the link between epithelial-mesenchymal transition and the cancer stem cell phenotype: a mathematical approach *J. Theor. Biol.* **265** 329–35
- [100] Ben-Jacob E, Coffey D S and Levine H 2012 Bacterial survival strategies suggest rethinking cancer cooperativity *Trends Microbiol.* **20** 403–10